Geochemical Perspectives Letters

Constant iron isotope composition of the upper continental crust over the past 3 Gyr

X.-M. Liu, R.M. Gaschnig, R.L. Rudnick, R.M. Hazen, A. Shahar

Supplementary Information

The Supplementary Information includes:

- Analytical Methods
- Tables S-1 to S-3
- Figure S-1
- Supplementary Information References

Analytical Methods

All iron isotope preparation and analyses were performed at the Carnegie Institution for Science. A brief description of sample dissolution, column chemistry and instrumental analysis is provided below and details are included in supplementary text. Around 5–20 mg of powder samples were dissolved using a combination of HF-HNO_3-HCl acids (3:1:1), and flux twice with NHO_3. After dissolution, rock solutions were dried down in Teflon beakers and dissolved in 6M HCl for column separation. We followed the column procedure of Dauphas *et al*. (2009), where 1 mL of stock solutions were taken to go through column chemistry packed with 1 mL of Bio-Rad Analytical Grade (AG)1-X8 200-400 mesh anion-exchange resins. These resins were pre-cleaned and conditioned with 10 mL of Milli-Q® H_2O, 5 mL of 1 M HNO_3, 10 mL of H_2O, 10 mL of 0.4 M HCl, 5 mL of H_2O, and 2 mL of 6 M HCl in succession. Sample solutions were loaded to the columns in 1 mL of 6 M HCl. Matrix elements were eluted in 8 mL of 6 M HCl, in a sequence of 0.5-, 0.5-, 1-, 2-, and 4- mL. Iron cuts were then eluted out in 9 mL of 0.4 M HCl, in a sequence of 0.5-, 0.5-, 1-, 3-, and

4-mL final solution for instrumental analysis. Finally, purified Fe solutions (~4 ppm Fe in 0.4M HNO_3) were analysed using a Nu Plasma II Multi Collector-Inductively Coupled Plasma-Mass Spectrometer (MC–ICP–MS). High mass resolution (HR) mode is used to reduce isobaric interferences. Even in HR mode, there may be unresolved Cr interference on Fe. Thus, we adopt a Cr correction method due to its possible isobaric inference on ^{54}Fe as follows. The β is calculated for the sample or standard based on the $^{57}Fe/^{56}Fe$ ratios. This β is then used to compute fractionated $^{54}Cr/^{53}Cr$ assuming that $\beta_{Cr} = \beta_{Fe}$ and using unfractionated ratios $^{54}Cr/^{53}Cr$=0.24890 (Shield *et al.*, 1966). The fractionated $^{54}Cr/^{53}Cr$ ratios were then combined with measured ^{53}Cr intensities to subtract isobaric interferences on ^{54}Fe.

Background signals for ^{56}Fe ($<10^{-4}$ V) were negligible compared to the typical sample signals (5–7 V). Standard bracketing, using IRMM524a (made from IRMM® certified Reference iron foil), was performed for all analyses. The Fe isotope composition of IRMM524a is identical from that of previously used international standard, IRMM-014. Therefore, the Fe isotope composition is reported as $\delta^{56}Fe$, where $\delta^{56}Fe_{sample} = [(^{56}Fe/^{54}Fe)_{sample}/(^{56}Fe/^{54}Fe)_{IRMM\text{-}014} - 1] \times 1000$. The external precision of $\delta^{56}Fe$ was evaluated by repeatedly running two USGS rock standards, BIR-1 (Icelandic basalt) and MAG-1 (Marine mud), respectively (Table S-2). BIR-1 yielded $\delta^{56}Fe$ of 0.05 ± 0.03 ‰ (2σ, n= 5) cf. 0.03 to 0.06 ‰ in the literature (GeoReM database: http://georem.mpch-mainz.gwdg.de/), and MAG-1 yielded $\delta^{56}Fe$ of 0.11 ± 0.04 ‰ (2σ, n = 5) cf. 0.09 to 0.13‰ in the literature (GeoReM database).

Supplementary Tables

Table S-1 Fe isotope data with age, location and major element information.

Sample ID	Stratigraphic unit	Unit(s)	Location	Sample number	Depositional Age	Relative to GOE	$\delta^{56}Fe$	$\delta^{57}Fe$	SiO_2	TiO_2	Al_2O_3	Fe_2O_3T	MnO	MgO	CaO	Na_2O	K_2O	P_2O_5	LOI[a]	TOC[b]	CIA[c]
					(Ma)		(‰)	(‰)	wt.%	wt.%	wt.%	wt.%	wt.%	wt.%	wt.%	wt.%	wt.%	wt.%	wt.%	wt.%	
Bolivia	Palaeozoic	Mandiyuti and Machareti Groups	Bolivia	6	315	post	0.14	0.20	73.61	0.62	12.29	3.87	0.05	1.58	0.40	1.10	2.80	0.12	3.56	0.25	70
Dwyka East	Palaeozoic	Dwyka Group, eastern outcrops	South Africa	8	300	post	0.08	0.14	67.26	0.64	13.87	5.41	0.09	2.29	1.57	3.16	2.96	0.18	2.58	0.19	56
Dwyka West	Palaeozoic	Dwyka Group, western drill core	South Africa	8	300	post	-0.25	-0.35	42.80	0.44	8.76	9.77	0.70	8.01	10.40	0.90	1.72	0.13	16.36	0.37	65
		Dwyka Group, western drill core					-0.22	-0.33													
Gaskiers	Neoproterozoic	Gaskiers Formation	Newfoundland	4	580	post	0.09	0.15	66.76	0.68	14.91	5.18	0.11	1.66	1.15	3.57	3.27	0.14	2.58	0.05	57
Nantuo	Neoproterozoic	Nantuo Formation	China	10	645	post	0.13	0.16	65.15	0.61	14.29	5.64	0.13	2.40	1.82	1.26	3.30	0.12	5.28	0.04	65
Gucheng	Neoproterozoic	Gucheng Formation	China	5	680	post	0.15	0.22	66.49	0.62	14.29	5.36	0.66	2.05	1.10	1.03	3.37	0.14	4.89	0.03	67
Blaubeker	Neoproterozoic	Blaubeker Formation	Namibia	6	630	post	0.23	0.36	76.85	0.49	9.87	3.90	0.05	1.35	0.55	1.67	3.07	0.12	2.08	0.08	59
Numees	Neoproterozoic	Numees Formation	Namibia	8	650	post	0.17	0.15	70.68	0.47	12.64	3.71	0.07	1.51	1.93	1.97	3.91	0.16	2.96	0.15	54
Ghaub	Neoproterozoic	Ghaub Formation	Namibia	3	635	post	0.09	0.11	32.01	0.35	7.23	3.35	0.05	3.00	26.86	0.60	2.18	0.14	24.23	0.03	64
Kaigas	Neoproterozoic	Kaigas Formation	Namibia	5	755	post	0.16	0.24	63.84	0.78	15.12	6.07	0.10	2.38	2.20	2.62	3.33	0.19	3.37	0.06	57
Chuos	Neoproterozoic	Chuos Formation	Namibia	5	690	post	0.22	0.37	47.07	0.45	8.28	7.41	0.75	6.45	10.72	1.13	2.39	0.22	15.13	0.11	58
		Chuos Formation					0.20	0.30													
Pocatello	Neoproterozoic	Pocatello Formation	Idaho	6	685	post	-0.06	-0.08	69.29	1.10	12.70	6.34	0.08	1.68	0.74	1.05	3.84	0.26	2.91	0.09	66
		Pocatello Formation					-0.03	0.06													
Konnarock	Neoproterozoic	Konnarock Formation	Virginia	5	665	post	0.11	0.23	67.54	0.74	13.97	5.24	0.08	1.50	1.20	2.69	4.44	0.21	2.40	0.09	56
Gowganda	Palaeoproterozoic	Gowganda Formation, Huronian Supergroup	Ontario	16	2350	syn	0.13	0.17	65.84	0.54	14.71	6.36	0.07	2.60	0.93	4.64	2.00	0.14	2.18	0.04	57
Bruce	Palaeoproterozoic	Bruce Formation, Huronian Supergroup	Ontario	3	2380	syn	0.12	0.17	67.88	0.46	14.77	4.55	0.02	3.20	0.35	3.72	2.71	0.10	2.25	0.03	61
Ramsay Lake	Palaeoproterozoic	Ramsay Formation, Huronian Supergroup	Ontario	5	2436	pre	0.08	0.17	67.91	0.55	12.68	7.73	0.10	3.23	1.02	1.44	2.08	0.14	3.12	0.04	67
Bottle Creek	Palaeoproterozoic	Bottle Creek Formation, Snowy Pass Supergroup	Wyoming	4	2275	syn	0.08	0.14	71.01	0.45	13.33	4.19	0.05	2.50	0.52	4.15	1.91	0.12	1.77	0.04	58
Makganyene	Palaeoproterozoic	Makganyene Formation	South Africa	6	2436	pre	-0.58	-0.98	56.69	0.38	8.30	18.45	0.39	3.96	3.36	0.06	1.01	0.09	7.31	0.17	89
	Palaeoproterozoic	Makganyene Formation					-0.59	-0.75													
Duitschland	Palaeoproterozoic	Duitschland Formation, Transvaal Supergroup	South Africa	5	2350	syn	-0.01	0.05	55.09	0.70	14.67	12.02	0.29	2.73	2.87	0.08	3.00	0.14	8.41	0.18	82
Timeball Hill	Palaeoproterozoic	Timeball Hill Formation, Transvaal Supergroup	South Africa	6	2300	syn	0.09	0.17	64.99	0.55	15.51	7.52	0.07	1.61	1.58	1.37	3.19	0.15	3.46	0.13	66
Mozaan	Mesoarchean	Mozaan Group, Pongola Supergroup	South Africa	7	2965	pre	0.19	0.28	57.24	0.37	8.70	25.05	0.13	3.00	0.44	0.55	1.40	0.06	3.07	0.02	74
Afrikander	Mesoarchean	Lagerspoort diamictite	South Africa	4	2960	pre	0.12	0.13	63.28	0.24	8.45	8.40	0.14	9.31	6.04	0.56	0.59	0.04	2.95	0.03	77
Coronation	Mesoarchean	Coronation Formation, Witwitarsrand Supergroup	South Africa	5	2960	pre	0.20	0.33	72.04	0.49	14.79	4.04	0.05	1.92	0.36	0.32	2.87	0.07	3.05	0.05	78
		Coronation Formation, Witwitarsrand Supergroup					0.23	0.40													
Promise	Mesoarchean	Promise Formation, Witwitarsrand Supergroup	South Africa	3	2960	pre	0.16	0.21	70.30	0.38	11.04	9.51	0.08	2.65	0.80	0.64	1.47	0.04	3.10	0.05	75

Note: Major element data are from Gaschnig *et al*. (2016).
[a] LOI = loss on ignition.
[b] TOC from Greaney *et al*. (2020).
[c] CIA (Chemical Index of Alteration) = $Al_2O_3/(Al_2O_3 + CaO + Na_2O + K_2O) \times 100$ (in molar ratio).

Table S-2 Accuracy evaluation based on two USGS standards.

Sample name	Sample description	δ^{56}Fe	δ^{57}Fe	δ^{56}Fe GEOREM
USGS BIR-1	Icelandic basalt	0.06	0.08	
USGS BIR-1	Icelandic basalt	0.05	0.10	
USGS BIR-1	Icelandic basalt	0.04	0.04	
USGS BIR-1	Icelandic basalt	0.07	0.08	
USGS BIR-1	Icelandic basalt	0.03	0.09	
	Average	**0.05**	**0.08**	***0.05***
	2 s.d.	0.03	0.04	
USGS MAG-1	Marine mud powder	0.08	0.11	
USGS MAG-1	Marine mud powder	0.11	0.12	
USGS MAG-1	Marine mud powder	0.09	0.13	
USGS MAG-1	Marine mud powder	0.12	0.18	
USGS MAG-1	Marine mud powder	0.14	0.12	
	Average	**0.11**	**0.13**	***0.11***
	2 s.d.	0.04	0.06	

Table S-3 Mineralogy of the diamictite composites as determined by X-ray diffraction.

	quartz	plagioclase	chlorite	muscovite	biotite	amphibole	calcite	dolomite-ankerite	siderite	hematite	magnetite	corundum	titanite	Fe mineral (%)
Bolivian	55.13	9.39	6.71	21.87	0.00	0.00	0,40	0.00	0.00	0.00	0.00	0.00	0.00	6.71
Dwywa East	34.75	30.90	14.02	9.24	0.00	0.00	0.00	0.00	0.00	0.00	0.00	0.00	0.00	14.02
Dwyka West	25.32	7.64	17.39	8.41	0.00	0.00	7.62	22.82	0.00	0.77	0.00	0.00	0.00	18.16
Newfoundland	32.08	35.36	5.48	21.23	0.00	0.00	0.00	0.00	0.00	0.00	0.00	0.00	0.00	5.48
Nantuo	42.77	12.14	9.75	30.46	0.00	0.00	0.23	0.00	0.00	0.00	0.00	0.00	0.00	9.75
Gucheng	46.85	12.02	8.22	31.64	0.00	0.00	0.41	0.00	0.00	0.00	0.00	0.00	0.00	8.22
Blaubeker	55.64	15.66	7.82	10.31	0.00	0.00	0.48	0.00	0.00	0.00	0.00	0.00	0.00	7.82
Numees	46.89	17.44	1.91	21.94	5.19	0.00	2.17	0.00	0.00	0.00	0.00	0.00	0.00	7.10
Ghaub	17.53	5.81	2.61	16.53	5.11	0.00	46.07	6.33	0.00	0.00	0.00	0.00	0.00	7.72
Kaigas	33.82	23.65	6.54	24.62	5.68	0.00	2.15	0.00	0.00	0.00	0.00	0.00	0.00	12.22
Chuos	30.29	10.88	5.38	11.70	8.30	0.00	6.72	22.71	0.00	0.00	0.00	0.00	0.00	13.68
Pocatello, Idaho	47.65	9.68	3.11	35.35	0.00	0.00	0.00	0.00	0.00	1.58	0.00	0.00	0.00	4.69
Konnarock	36.81	24.76	1.97	22.36	0.00	0.00	0.73	0.00	0.00	2.36	0.00	0.00	0.00	4.33
Gowganda	28.28	39.83	9.74	8.86	2.55	2.13	0.38	0.00	0.00	0.00	0.00	0.00	0.00	14.42
Bruce	33.70	33.00	12.69	8.74	0.00	0.00	0.00	0.00	0.00	0.00	0.00	0.00	0.00	12.69
Ramsay Lake	47.25	10.96	14.21	12.56	5.49	0.00	0.99	0.00	0.00	0.00	0.00	0.00	0.00	19.70
Bottle Creek	40.68	36.37	5.32	9.17	8.01	0.00	0.00	0.00	0.00	0.00	0.00	0.00	0.00	13,33
Makganyene														0.00
Duitschland	40.50	0.00	13.57	31.84	0.00	0.00	0.00	8.92	3.55	0.00	0.00	0.00	0.00	17.12
Timeball Hill	38.02	11.07	10.25	25.58	0.00	0.00	0.89	0.00	0.00	0.00	0.00	11.36	0.00	10.25
Pongola	52.02	4.16	23.17	0.00	4.27	0.00	0.00	0.00	0.00	0.00	7.02	0.00	0.00	34.46
Lagerspoort	41.65	5.32	19.33	0.00	0.00	28.43	0.00	0.57	0.00	0.00	0.00	0.00	0.00	47.76
Coronation	60.33	0.00	8.47	29.02	0.00	0.00	0.25	0.00	0.00	0.00	0.00	0.00	0.00	8.47
Promise														

Note: The XRD analyses were performed at the Mineralogy Facility, Indiana University Bloomington, where X-ray diffraction patterns were determined using a Bruker D8 Advance X-Ray Powder Diffractometer. The XRD patterns were analysed using Rietveld refinement (Rietveld, 1969; Bish and Post, 1993) with TOpas (Bruker AXS) software to determine mineral abundances.

Supplementary Figures

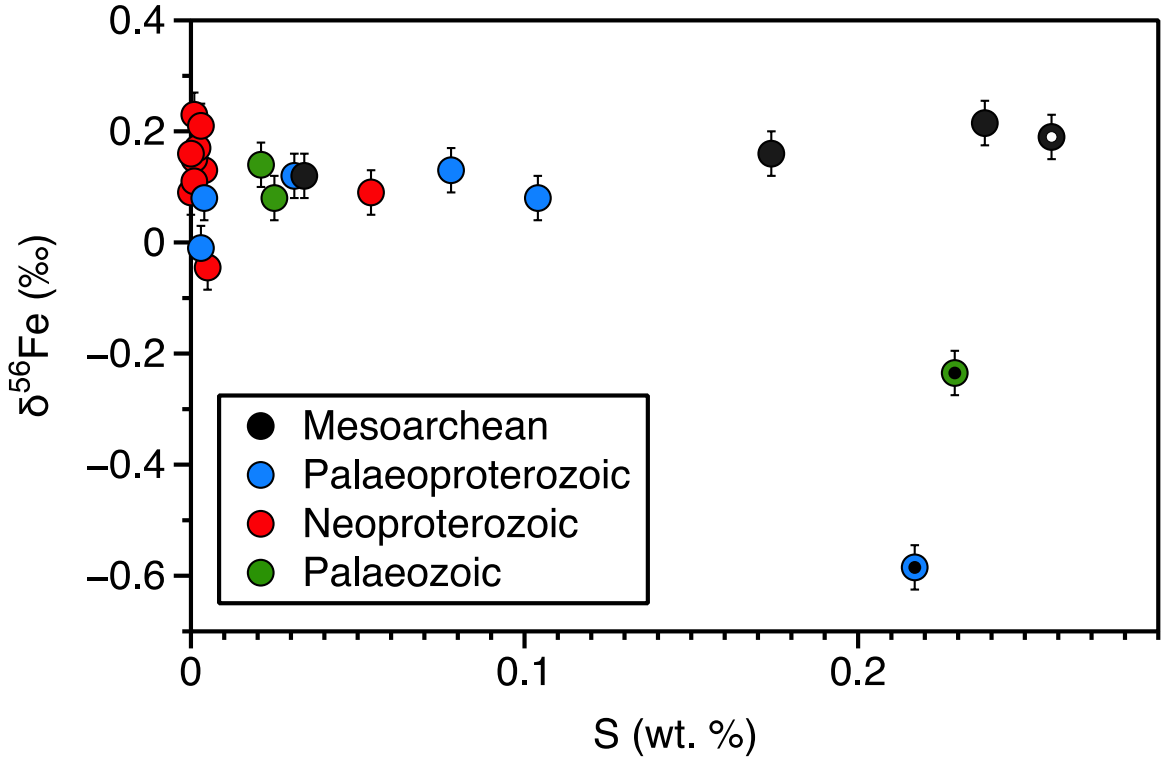

Figure S-1 δ^{56}Fe plots against total sulfur content (wt. %) in all diamictite composites. Black lines denote linear fit with blue field indicating 95 % confidence interval of fitting.

Supplementary Information References

Bish, D.L., Post, J.E. (1993) Quantitative mineralogical analysis using the Rietveld full-pattern fitting method. *American Mineralogist* 78, 932–940. http://www.minsocam.org/ammin/AM78/AM78_932.pdf

Dauphas, N., Craddock, P.R., Asimow, P.D., Bennett, V.C., Nutman, A.P., Ohnenstetter, D. (2009) Iron isotopes may reveal the redox conditions of mantle melting from Archean to Present. *Earth and Planetary Science Letters* 288, 255–267. https://doi.org/10.1016/j.epsl.2009.09.029

Gaschnig, R.M., Rudnick, R.L., McDonough, W.F., Kaufman, A.J., Valley, J.W., Hu, Z., Gao, S., Beck, M.L. (2016) Compositional evolution of the upper continental crust through time, as constrained by ancient glacial diamictites. *Geochimica et Cosmochimica Acta* 186, 316–343. https://doi.org/10.1016/j.gca.2016.03.020

Greaney, A.T., Rudnick, R.L., Romaniello, S.J., Johnson, A.C., Gaschnig, R.M., Anbar, A.D. (2020) Molybdenum isotope fractionation in glacial diamictites tracks the onset of oxidative weathering of the continental crust. *Earth and Planetary Science Letters* 534, 116083. https://doi.org/10.1016/j.epsl.2020.116083

Rietveld, H.M. (1969) A profile refinement method for nuclear and magnetic structures. *Journal of Applied Crystallography* 2, 65–71. https://doi.org/10.1107/S0021889869006558

Shields, W.R., Murphy, T.J., Catanzaro, E.J., Garner, E.L. (1966) Absolute isotopic abundance ratios and the atomic weight of a reference sample of chromium. *Journal of Research of the National Bureau of Standards. Section A, Physics and Chemistry* 70A, 193–197. https://doi.org/10.6028/jres.070A.016